



# Shear Capacity of Lightweight Concrete Beam Reinforced with Glass Fiber-Reinforced Polymer Bars

Habib Akbarzadeh Bengar<sup>1</sup> · Fatemeh Ahmadi Zarrinkolaei<sup>2</sup> · Mohsen Bozorgnasab<sup>1</sup>

Received: 17 December 2019 / Accepted: 15 August 2020 / Published online: 27 August 2020  
© Shiraz University 2020

## Abstract

In this article, the shear behavior of lightweight concrete beams reinforced with glass fiber-reinforced polymer (GFRP) bars is examined. Here, in order to investigate the effect of bar type on the shear strength, the GFRP bar was used as the longitudinal bar. In total, eight concrete beams with a span length of 2 m and section dimensions of 150 × 250 mm without transverse reinforcement were tested. The parameters under study included the concrete type (lightweight and conventional), shear spans-to-depth ratio ( $\frac{a}{d}$ ) (2.5 and 4), bar type (steel and GFRP), and diameter of the longitudinal bars (12 and 16 mm). The results of the tests showed that the failure of the beams under study was of the shear type, as expected. With an increase in the  $\frac{a}{d}$  ratio, the shear strength decreased, and more flexural cracks were observed. The shear strength of the lightweight concrete beams was obtained lower than that of the corresponding conventional concrete beams. The beams reinforced with the steel bars demonstrated a higher stiffness relative to the ones reinforced with the GFRP bars. Furthermore, the shear strength results obtained from the tests were compared with those predicted by equations proposed by several codes as well as studies in the literature. The comparison showed good consistency of the experimental results with those predicted by the Canadian code.

**Keywords** RC beams · Shear strength · Lightweight concrete · GFRP

## 1 Introduction

A significant challenge faced by structural designers is issues associated with the heavy weight or dead load of a reinforced concrete structure. One of the main approaches to address this problem is the use of lightweight concrete. Structural lightweight concretes have a compressive strength above 17 MPa despite having a density of less than 2000 kg/m<sup>3</sup>. The manufacture of these concretes is only possible through the use of lightweight and strong aggregate. The maximum strength of lightweight aggregate concrete is accomplished

when lightweight aggregate with a strength greater than or equal to that of the concrete matrix is used for lightweight construction (Chung et al. 2018; Naseri et al. 2019; Real et al. 2017; Yazdani and Goucher 2015).

The application of lightweight concrete in structural elements and systems leads to a lower cost of the foundation and structure, and it also provides a better thermal and sound insulation compared with concrete with normal density. The applicability of lightweight concrete depends on the properties required in terms of the volumetric weight, strength, and heat transfer capacity (Askari Dolatabad et al. 2019; Chung et al. 2018; Gonen 2015).

The same creep values were seen for the two lightweight and conventional concrete types having equal compressive strength. The tensile strength and modulus of elasticity of lightweight concrete are 25–50% lower than the corresponding values of the conventional concrete; thus, larger deformations are obtained for lightweight concrete. However, the resistance of lightweight concrete to fire and freeze–thaw cycles is higher, due to a greater porosity of lightweight aggregate (Mousavinejad and Sara 2019; Nilson and Martinez 1986).

✉ Habib Akbarzadeh Bengar  
h.akbarzadeh@umz.ac.ir

Fatemeh Ahmadi Zarrinkolaei  
ahmadi\_zarrin17@yahoo.com

Mohsen Bozorgnasab  
m.bozorgnasab@umz.ac.ir

<sup>1</sup> Department of Civil Engineering, University of Mazandaran, Babolsar, Iran

<sup>2</sup> Department of Civil Engineering, Mazandaran University of Science and Technology, Babol, Iran

Previous studies addressed the mechanical properties, flexural behavior, and bond strength of lightweight aggregate (LWA) concrete (Akbarzadeh Bengar et al. 2020a, b; Limbachiya et al. 2012; Nematzadeh et al. 2020; Shafiqh et al. 2014; Tang et al. 2009). Nevertheless, the literature lacks research focusing on the shear behavior and strength of reinforced LWA concrete beams. LWA type impacts the aggregate interlocking, as a major factor in the shear strength of concrete. In addition, the shear failure is a brittle, catastrophic failure (Xu et al. 2018; Bompa and Elghazouli 2015; Campana et al. 2013). Multiple empirical works in the literature addressing the shear performance of LWA indicated that the LWA type including oil palm and palm kernel shell aggregates impacted the aggregate interlocking (Alengaram et al. 2011). Therefore, prior to using such LWA types in building RC members, the concrete shear strength,  $V_c$ , and behavior of shear-deficient RC beams containing LWA must be investigated. Multiple factors affect the shear strength of RC beams, which include the compressive strength of concrete, shear span-to-depth ratio ( $a/d$ ), shear reinforcement (stirrups), maximum aggregate diameter, and bond strength in the transition zone. In a study by Jumaat et al. (2009), RC beams made with oil palm LWA, having a compressive strength and density of 20 MPa and 1650 kg/m<sup>3</sup>, respectively, were tested, and the results indicated that the shear capacity of these beams was 10% greater than that of those made with normal-weight concrete (NWC). Alengaram et al. (2011) conducted a similar study on the shear performance and strength of RC beams made with palm kernel shell aggregate, where eight beams were subjected to four-point bending. It was found that the shear strength of the beams made with LWA was greater than that made with NWA by 24%. The shear strength values of lightweight concrete (LWC) specimens obtained in the above studies (Alengaram et al. 2011; Jumaat et al. 2009) were greater than those of specimens made with NWC by 10–24%. This was attributed to the shorter and narrower cracks with rougher surfaces developed in LWC beam specimens, which in turn improved the shear strength of these beams. According to the findings, in comparison with NWC, LWC beams demonstrated better behavior in terms of crack spacing and aggregate interlocking.

Over the past century, numerous concrete structures reinforced with steel have been constructed to serve as infrastructures. Some of these structures, such as parking garages, bridges, and water tanks, are exposed to harsh environmental conditions, leading to the corrosion of steel and the subsequent deterioration of concrete. This results in higher maintenance costs and reduced service life of a structure (Dhahir 2017; Omeman et al. 2008; Tureyen and Froesch 2002). The problem of steel corrosion reduces the service life, and solutions such as a concrete cover also lead to additional costs. Recent technological developments

have led to the discovery of potential reinforcing materials such as a fiber-reinforced polymer (FRP) which can be produced in the form of bars or plates (Akbarzadeh Bengar 2015; Akbarzadeh Bengar et al. 2020a, b; Akbarzadeh Bengar and Maghsoudi 2010; 2011; Akbarzadeh Bengar and Shahmansouri 2020; Azarm et al. 2017; Bhuvaneshwari and Mohan 2017; Farrokh Ghatte 2020; Farrokh Ghatte et al. 2019; Ghasemi et al. 2015; Hosseinpour et al. 2019; Kaveh et al. 2017; Maghsoudi and Akbarzadeh Bengar 2011a, b; Shayanfar and Akbarzadeh Bengar 2018). These materials are incorporated inside concrete members to provide supplementary desired properties. Therefore, a strategy to avoid corrosion is to use concrete reinforced with FRP bars. FRP composites are known to have properties including high tensile strength, high strength-to-weight ratio, corrosion resistance, electrical non-conductivity, lightweight (around a quarter of the weight of steel bars), easy installation, and adaptability. These properties have made this material type an interesting and appropriate option for modern construction purposes (ACI Committee 2015; GangaRao et al. 2006; Singh 2015).

In case of employing FRP as the reinforcement, one must note that it possesses a somewhat small modulus of elasticity, a high tensile strength without a yielding point, a considerably lower tensile strength in the bent portion relative to the straight portion, and a small dowel resistance. The modulus of elasticity of CFRP (carbon fiber-reinforced polymer) bars is much higher than that of the GFRP (glass fiber-reinforced polymer) bars (GangaRao et al. 2006; Hajiloo et al. 2018; Oskouei et al. 2017; Said et al. 2016; Saleh et al. 2019; Singh 2015; Wu et al. 2016; Yazdanbakhsh and Tian 2019; Zhou et al. 2017).

Despite the extensive research conducted over recent decades, the accurate determination of the shear capacity of concrete structures remains a difficult task. The shear design of standard codes currently in practice is still based on the semi-experimental shear design method proposed by the ACI-ASCE Committee in 1962 (ACI-ASCE Committee 326 1962). However, an entirely reasonable design method is available for determining the flexural capacity of reinforced concrete (RC) members (ACI Committee 2014; BSI 1997; Canadian Standards Association 2016; CEN European Committee for Standardization 2004; Shoib et al. 2015). One of the main reasons behind the weakness of the shear design regulations for RC members is the fact that shear failure is a complicated phenomenon that is affected by a large number of parameters, probably even more than 20 parameters, as proposed by Leonhard (1970). These parameters depend on the behavior of the shear cracks in the concrete in the nonlinear stage.

Research has shown that FRP composites delay the growth of critical diagonal cracks to a great extent and significantly improve the load-carrying capacity of RC beams.

However, concrete beams reinforced with FRP bars without transverse reinforcement show a lower shear strength relative to beams reinforced with steel bars (ACI Committee 2015; Zhang et al. 2015). On the other hand, the shear strength of lightweight concrete is smaller than that of conventional concrete (ACI Committee 2014; Shoaib et al. 2015).

Due to its high permeability, harmful and corrosive substances penetrate the matrix of lightweight concrete; therefore, in environments where the corrosion of ordinary steel bars is possible, FRP bars should be used for reinforcement. In this study, experimental work was performed to investigate and compare the shear strengths of lightweight and conventional concrete beams reinforced with steel and GFRP bars. During the research procedure, the cracking pattern, type of failure, and effect of the shear span were briefly addressed, and the shear behavior was investigated using the load–deflection diagram. Besides, the obtained results were compared with those of equations proposed in four standard codes and guidelines (ACI Committee 2015; Canadian Standards Association 2016; El-Sayed et al. 2006; JSCE 1997).

## 2 Experimental Program

### 2.1 Materials

To produce the lightweight concrete in this work, light expanded clay aggregate (LECA) was utilized as the lightweight aggregate. The bulk density of the LECA particles was 330–430 kg/m<sup>3</sup>. LECA with particles varying in size from 4 to 10 mm was used as the coarse aggregate, and sand was used as the fine aggregate. Water absorption for the sand and LECA was 3 and 24%, respectively. A third-generation superplasticizer commercially available as FRD-B305 was used, with the related information given in Table 1. Type II Portland cement and micro-silica (silica fume) were used here as the binders, the details of which are presented in Table 2. In this study, the deformed steel bar was used. The details of the steel and GFRP bars are given

**Table 1** Properties of superplasticizer

Type of superplasticizer	Color	Density (kg/m <sup>3</sup> )	pH
Superplasticizer (FRD-B305)	Brown color fluid	1200	7

**Table 2** Chemical properties of binders (%)

Cement materials	SiO <sub>2</sub>	Fe <sub>2</sub> O <sub>3</sub>	Al <sub>2</sub> O <sub>3</sub>	CaO	MgO	Na <sub>2</sub> O	K <sub>2</sub> O	P <sub>2</sub> O	SO <sub>3</sub>	LiO
Micro-silica	96.4	0.87	1.32	0.49	0.97	0.31	1.01	0.16	0.1	–
Cement	22	3.2	4.44	64.9	1.42	0.27	0.58	–	1.67	1.3

in Table 3. The data in the above tables were obtained from the manufacturer.

### 2.2 Mixture Properties

Here, two concrete types, namely conventional (normal) and lightweight concretes, were used, for which the mix design data are given in Table 4. Conventional concrete was prepared as the reference concrete for comparison. The water-to-cementitious materials ratio was selected as 0.5 and 0.44 for the conventional and lightweight concretes, respectively. The slump for both types of concretes was constant and equal to 80 mm. The density of the conventional and lightweight concretes was 2350 and 1800 kg/m<sup>3</sup>, respectively. Both concrete types had the same 28-day compressive strength of 21 MPa.

### 2.3 Specimens and Test Procedure

In this research, eight reinforced concrete beams consisting of lightweight and conventional concrete beams were manufactured with a span length and cross-sectional area of 200 cm and 375 cm<sup>2</sup>, respectively. The loading was applied in the form of two concentrated loads acting on the beams with two different shear spans-to-depth ratios ( $\frac{a}{d} = 2.5$  and 4). The beams had two longitudinal bars in the tensile zone, and to explore the shear strength as well as the shear failure of the lightweight concrete reinforced with GFRP bars, the beams were made without transverse reinforcement. The concrete cover thickness surrounding the bars was 5 cm.

The IDs assigned to the specimens consist of four parts; the first part indicates the bar type (G for GFRP and S for steel); the second part denotes the concrete type (N for normal (conventional) and L for lightweight); the third part expresses the diameter of the two bars in each beam (D12 for 12 mm and D16 for 16 mm bars); and the fourth part shows the shear span-to-effective depth ratio (2.5 and 4). The details of the beams under study are presented in Table 5.

**Table 3** Mechanical properties of GFRP and steel materials

Rebar type	Tensile strength (MPa)	Tensile modulus (GPa)	Tensile strain (%)
GFRP	1000	66.4	1.51
Steel	600	200	14

A schematic representation of the beams under study as well as the loading system is shown in Fig. 1. The four-point flexural test was conducted on the specimens. A 400-KN universal testing machine (UTM) was used for loading which was performed in a load-controlled manner. During the testing, the force and mid-span deflection were measured and recorded by data loggers.

In order to accurately examine the beams under study and to investigate the effect of the considered variables, the load–deflection diagram of the beams at mid-span was plotted. The variables of interest included the type of concrete and type of bar, bar diameter, and the shear span-to-depth ratio ( $\frac{a}{d}$ ) of the beam.

### 3 Results and Discussion

Here, through extensive experimental work, the cracking pattern, failure mode, and concentrated applied load vs. mid-span deflection curve of the beams were investigated, and the shear capacity results of the tested beams were compared with those of the equations proposed by standard codes and guidelines.

#### 3.1 Cracking Pattern and Failure Mode

The cracking pattern is shown in Fig. 2, where it is seen that in the beams with the shear span-to-effective depth ratio of 2.5, flexural cracks were not significant, and in some of them, very shallow flexural cracks appeared before the formation of diagonal shear cracks, and most of these beams experienced a completely sudden failure. In these beams, as the load increased, first, flexural cracks appeared, and then,

**Table 4** Mixture proportions for lightweight and normal concretes ( $\text{kg/m}^3$ )

Concrete type	Cement	Micro-silica	Super-plasticizer	Water	Sand	Gravel	LECA	W/B	Density
Lightweight concrete	450	70	9	175	850	–	270	0.44	1824
Normal-weight concrete	300	–	–	150	1150	750	–	0.5	2350

**Table 5** Details of the specimens

Beam specimen	Concrete type	Rebar type	$\rho$ (%)	$a$ (mm)	$d$ (mm)	$a/d$
G-L-D12-2.5	Lightweight	GFRP	0.75	500	200	2.5
G-L-D12-4	Lightweight	GFRP	0.75	800	200	4
G-L-D16-2.5	Lightweight	GFRP	1.34	500	200	2.5
G-L-D16-4	Lightweight	GFRP	1.34	800	200	4
G-N-D12-4	Normal weight	GFRP	0.75	800	200	4
G-N-D16-2.5	Normal weight	GFRP	1.34	500	200	2.5
S-L-D16-2.5	Lightweight	Steel	1.34	500	200	2.5
S-L-D12-4	Lightweight	Steel	0.75	800	200	4

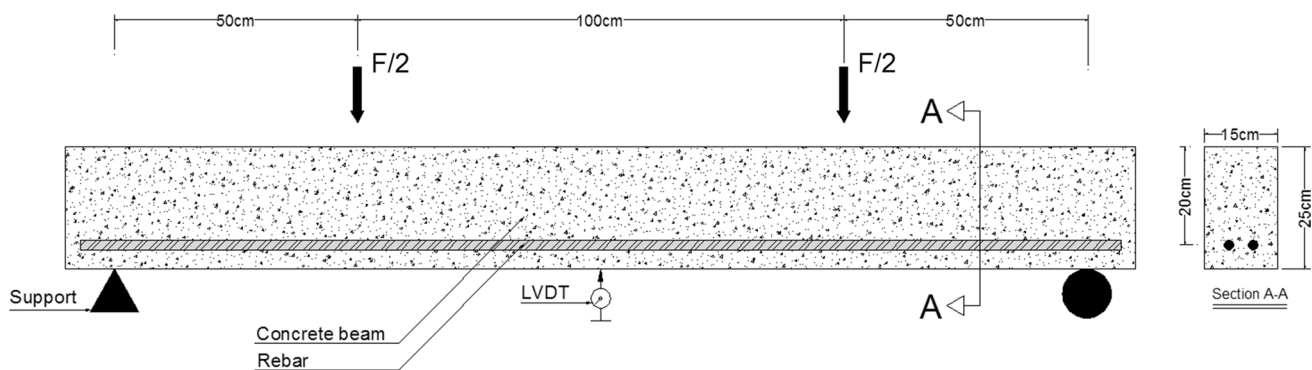
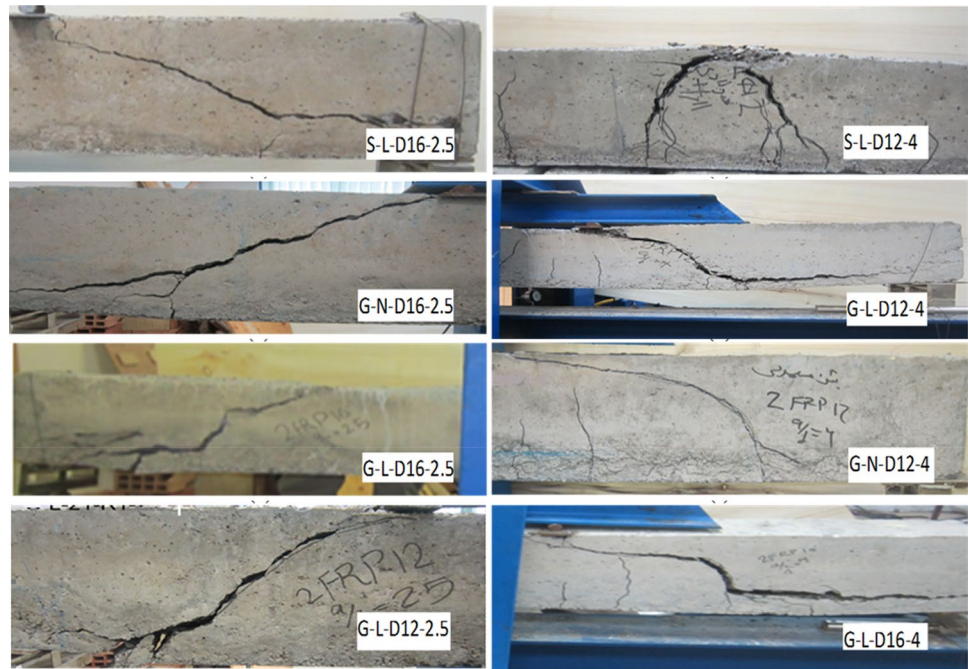


**Fig. 1** Schematic diagram of experimental beam specimens



**Fig. 2** The failure mode of beams



critical diagonal cracks with increasing width developed toward the supports, which led to the beam failure.

In the beams with the shear span-to-effective depth ratio of 4, the number of flexural cracks was significantly higher than that in beams with the shear span-to-effective depth ratio of 2.5. These flexural cracks extended from the bottom of the beam up to around the mid-height ( $0.5d$ ), and as the loading continued, the developed shear cracks led to the beam failure. Regarding the type and pattern of the cracks seen in the beams, in general, the failure of these beams was the result of the formation of flexural–shear cracks.

### 3.2 Load–deflection Behavior of the Tested Beams

Figure 3 demonstrates the shear force vs. mid-span deflection curve of the beams with  $\frac{a}{d} = 2.5$ . Regarding the curve, it can be found that in the early loading stages and before the appearance of microcracks, all beams demonstrate an almost equal stiffness. The similarity of the initial stiffness is due to the same cross-sectional area of the beams, and until the appearance of the first crack, the bars do not affect the stiffness. The beam G-L-D12-2.5 showed the highest post-cracking stiffness reduction, due to the formation of flexural cracks prior to shear ones.

As can be seen in Fig. 3, after the early loading stages, the steel bar-reinforced beam shows a stiffness greater than that of the other beams (having the GFRP bars), which is attributed to a higher modulus of elasticity of the steel bar relative to that of the GFRP bar. Comparing the curves of beams G-N-D16-2.5 and G-L-D16-2.5 shows that the lightweight concrete beam has a smaller stiffness relative to the

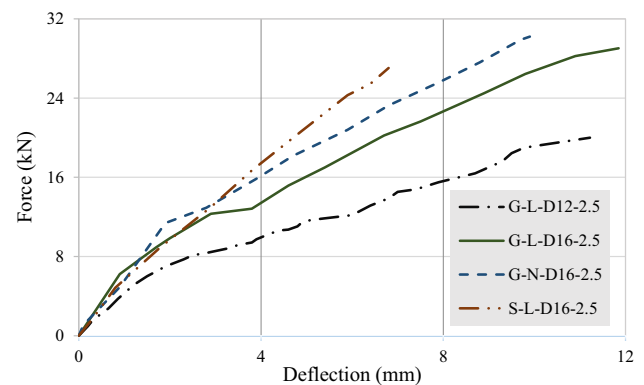


**Fig. 3** Beams with shear span/depth ratio of 2.5

conventional concrete beam, which is due to a lower modulus of elasticity of the lightweight concrete relative to the conventional concrete. Moreover, by comparing the shear force–deflection diagram of beams G-L-D12-2.5 and G-L-D16-2.5, it can be seen that the higher cross-sectional area of the longitudinal bar increases the beam stiffness; hence, despite the sudden shear failure of the beams, an increased cross-sectional area of the longitudinal bar led to a higher stiffness. Regarding the fact that the failure of all the beams under study was of shear mode due to shear cracks, as expected, the maximum applied load thus corresponded to the shear strength of the tested beams.

The shear force versus mid-span deflection behavior of the beams with  $\frac{a}{d} = 4$  is shown in Fig. 4. Due to the same cross section, all beams demonstrated an almost equal stiffness before cracking. After the appearance of the initial

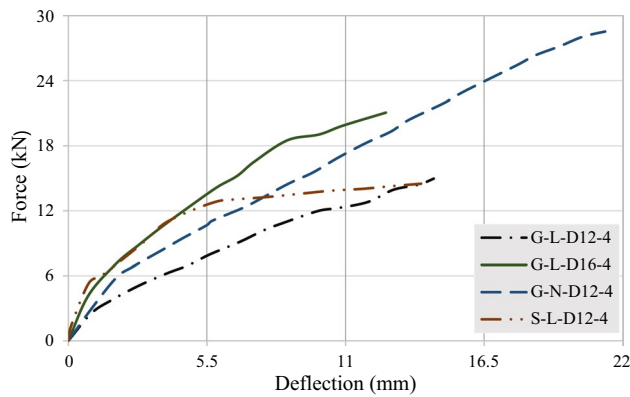


**Fig. 4** Beams with shear span/depth ratio of 4

flexural cracks, the stiffness of the beams saw a considerable reduction.

The stiffness of the beam G-L-D12-4 was less than that of the beam G-N-D12-4, which is attributed to the lower stiffness of the lightweight concrete relative to that of the conventional ones, as discussed above. In the lightweight concrete beams with  $\frac{a}{d} = 4$ , similar to the case with beams having  $\frac{a}{d} = 2.5$ , it was also seen that the beam reinforced with the steel bar (S-L-D12-4) demonstrated a higher stiffness relative to the one reinforced with the GFRP bar (G-L-D12-4), due to a higher modulus of elasticity of the steel bars. In the beams having the  $\frac{a}{d}$  ratio of 4, the cross-sectional area of the bars affected the beam's stiffness, with the beam G-L-D16-4 demonstrating a higher stiffness relative to the beam G-L-D12-4. It may be attributed to the higher cross-sectional area of the bars preventing the widening of cracks, which in turn prevents the stiffness reduction.

To further investigate the effect of shear span-to-effective depth ratio ( $\frac{a}{d}$ ) on the shear behavior of the beams, the load vs. mid-span deflection curves of the tested beams with different  $\frac{a}{d}$  ratios are given in Figs. 5 and 6. Figure 5 shows the curve of the lightweight concrete beams with the 12-mm-diameter GFRP bars, and Fig. 6 shows the curve of the same beams with the 16-mm-diameter GFRP bars. As can be seen in the figure, the beam with the higher  $\frac{a}{d}$  ratio demonstrates a lower stiffness after initial cracking. This observation is the result of the formation of more flexural cracks prior to the ultimate failure in the beam with the higher  $\frac{a}{d}$  ratio.

### 3.3 Shear Strength of Tested Beams

The results obtained from loading the beams are presented in Table 6. It can be seen from the table that the beam G-N-D16-2.5 with the equivalent force of 30 kN has the highest shear strength, and the beam G-N-D12-4 has the highest recorded deflection.

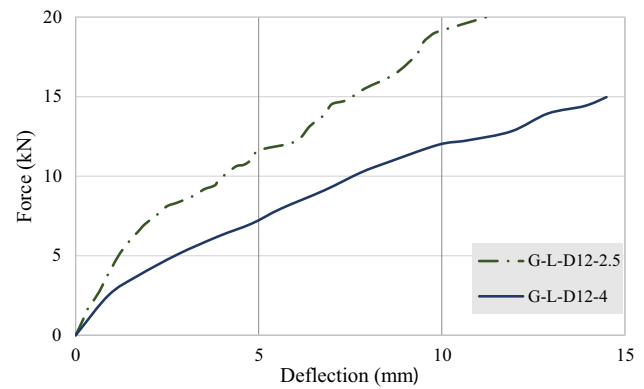


**Fig. 5** Effect of  $a/d$  ratio on shear behavior of beams with rebar diameter of 12 mm

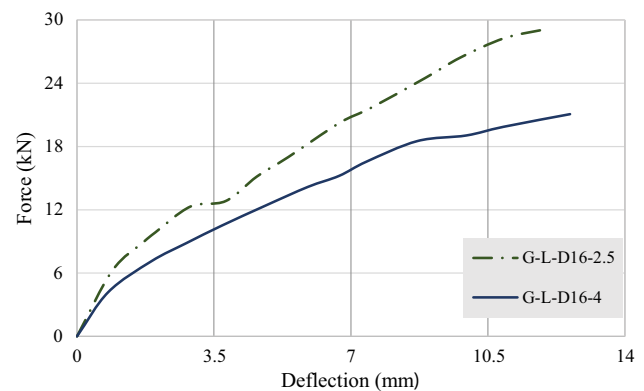


**Fig. 6** Effect of  $a/d$  ratio on shear behavior of beams with rebar diameter of 16 mm

**Table 6** Results of the test

Beam specimen	Max shear strength (kN)	Deflection in the middle of the beam (mm)	Failure mechanism
G-L-D12-2.5	20	11.7	Shear failure
G-L-D12-4	15	14.5	Shear failure
G-L-D16-2.5	29	11.8	Shear failure
G-L-D16-4	21	10.21	Shear failure
G-N-D12-4	28.5	21.3	Shear failure
G-N-D16-2.5	30	9.9	Shear failure
S-L-D16-2.5	27	6.85	Shear failure
S-L-D12-4	14.5	14	Shear failure

Considering the shear strength of beams G-L-D12-2.5 and G-L-D16-2.5, it is found that with 1.76 times increase in the cross-sectional area of the longitudinal bar, the shear strength of the beams increased by 45%. It was then concluded that a higher cross-sectional area of the longitudinal bars led to a higher shear capacity.

This phenomenon can be attributed to the fact that an increased cross-sectional area of the longitudinal bars delayed the propagation of the cracks and their progress toward the compressive region, which in turn led to greater shear strength. In addition, comparing the results of beams G-L-D12-4 and G-L-D16-4 shows that the GFRP bar with a greater cross-sectional area increased the shear strength of the beam by 40%, while this increase in the corresponding beams with  $\frac{a}{d} = 2.5$  was 45%.

The shear strength results of beams G-L-D16-2.5 and S-L-D16-2.5 indicate that the beam reinforced with the steel bars showed a relatively smaller (7%) shear strength relative to the beam with the GFRP bars despite having a higher stiffness, with the shear strength of beams G-L-D16-2.5 and S-L-D16-2.5 being 29 and 27 kN, respectively. Moreover, the shear strength values of beams S-L-D12-4 and G-L-D12-4 were almost equal. Regarding the reason behind this observation, it can be said that since the beams with steel bars have a flexural behavior with a large deflection, the strain of the steel bar reaches the yielding value, which results in more flexural cracks with a large width. This reduces the shear capacity of the section up to the point that the two beams with two types of rebars demonstrated an almost equal shear strength.

Comparing the results of beams G-N-D12-4 and G-L-D12-4 shows that the shear strength of the conventional (normal) concrete beam was much greater (40%) than that of the lightweight concrete beam. However, the shear strength results of beams G-L-D16-2.5 and G-N-D16-2.5 show a negligible difference (around 3%) between the shear strength values of the conventional and lightweight concretes, with

the corresponding shear strengths being 29 and 30 kN. The beams with  $\frac{a}{d} = 4$  experienced many flexural cracks before shear failure; in such a case, the shear strength of the beam depends on the shear strength of concrete in the compressive zone, aggregate interlock at crack faces, and dual-action behavior. Since LECA was used in the lightweight concrete beam, its shear strength was less than that of the beam with conventional concrete. On the other hand, the beams with  $\frac{a}{d} = 2.5$  experienced a few flexural cracks; thus, their shear strength depended on the un-cracked concrete. Since the concrete compressive strength was the same for the two beams with different shear span-to-effective length ratios, the same shear strength was obtained for the two concrete types.

### 3.4 Comparison of Experimental Results and shear Design Equations

The shear capacity of the tested beams was compared with the shear capacity proposed by methods presented in Table 7. As can be seen in the table, the theoretical equations for predicting the shear capacity of the lightweight and conventional concrete beams reinforced with GFRP bars consist of three equations proposed by different codes (ACI, JSCE, and CSA) as well as one equation proposed by previous researchers.

Table 7 demonstrates various models for the shear capacity of FRP-reinforced concrete beams,  $V_{cf}$ . ACI 440.1R-06 (ACI Committee 2015) hypothesizes that regarding the shear strength of FRP-reinforced beams, the effect that the dowel action of the FRP longitudinal bars has is smaller than that of an equivalent steel area. Table 7

**Table 7** Equations proposed by codes and researchers for predicting shear strength

Guideline	Equation
ACI 440.1R-06 (ACI Committee 2015)	$V_c = \frac{2}{5} \sqrt{f_c} b_w d$
El-Sayed et al. (2006)	$\text{where } c = kd \text{ and } k = \sqrt{\rho_f n_f + (\rho_f n_f)^2} - \rho_f n_f$ $V_{cf} = 0.037 \left( \frac{\rho_f E_f \sqrt{f_c}}{\beta_1} \right)^{\frac{1}{3}} b_w d \leq \frac{f_c}{6} b_w d$ $\text{where } 0.85 \geq \beta_1 = 0.85 - 0.007(f_c - 28) \geq 0.65$
JSCE (1997)	$V_{cf} = \frac{\beta_d \beta_p \beta_n f_{cvd} b_w d}{\gamma_b}$ $\text{where } f_{cvd} = 0.2(f_{cd})^{\frac{1}{3}} \leq 0.72 \text{ N/mm}^2$ $\beta_d = (1000/d)^{\frac{1}{4}} \leq 1.5$ $\beta_p = (1000 \rho_f E_f / E_s)^{\frac{1}{3}} \leq 1.5$ $\beta_n = 1 + M_0 / M_d \leq 2 \text{ for } N'_d \geq 0$ $\beta_n = 1 + 2M_0 / M_d \geq 0 \text{ for } N'_d < 0$
CAN/CSA-S806-02 (Canadian Standards Association 2016)	$V_{cf} = 0.035 \lambda \phi_c \left( f_c \rho_f E_f \frac{V_f}{M_f} d \right)^{1/3} b_w d$ $\text{such that: } 0.1 \leq \lambda \phi_c \sqrt{f_c} b_w d \leq V_{cf} \leq 0.2 \lambda \phi_c \sqrt{f_c} b_w d$

$b_w$ : width of the web of a beam;  $E_f$ : modulus of elasticity of FRP composite;  $f_c$ : specified compressive strength of concrete;  $\lambda$ : factor to account for concrete density;  $\phi_c$ : resistance factor for concrete

gives the concrete shear capacity,  $V_c$ , of flexural members where FRP is used as the main reinforcement. In the table,  $b_w$  is the web width,  $c$  is the neutral axis depth of the cracked transformed section, and  $\rho_f$  is the ratio of FRP reinforcing bars, with  $n_f$  being the modular ratio. The CAN/CSA-S806-02 (Canadian Standards Association 2016) and JSCE (1997) codes express the contribution that concrete has in the shear strength as the equations shown in Table 7. El-Sayed et al. (2006) reported that the ratio of the shear strength of FRP bar-reinforced concrete beams to that of steel bar-reinforced beams ( $V_{cf} / V_c$ ) is proportional to the cube root of the axial stiffness ratio of FRP to steel reinforcing bars ( $\sqrt[3]{\rho_f E_f / \rho_s E_s}$ ). This finding was applied to the shear design equation proposed by ACI 440.1R-03, leading to the new equation given in Table 7. To verify this equation, the shear strength results of 98 specimens tested to date were compared with those of the equation, and a good agreement was observed.

Table 8 reports the shear capacity results of the beams reinforced with GFRP bars predicted by the above methods. Regarding the table, it is found that the experimental results obtained here for the lightweight and conventional concrete beams reinforced with the GFRP bars show the most consistency with the Canadian Standard Association (CSA) code, with the results predicted by this code demonstrating the smallest difference with the experimental results obtained in this study. In the method proposed by this code, in addition to the concrete compressive strength and reinforcing bar ratio, the  $a/d$  ratio and modulus of FRP are also taken into account, which leads to more accurate results showing a greater agreement with the experimental results.

Comparing the experimental results with those of the proposed equations demonstrates that the theoretical and experimental results become closer to each other as the  $a/d$  ratio increases. For the smaller  $a/d$  ratio (the beams with  $a/d = 2.5$ ), the difference between the prediction and experimental results is greater and the behavior becomes similar to that of the deep beams, while the current codes address the conventional beams. For the beams with the same  $a/d$

ratio, greater consistency between the experimental and theoretical results is observed for the beams with the lower longitudinal bar ratio.

## 4 Conclusions

In this study, the shear behavior of lightweight concrete beams reinforced with GFRP bars and without transverse reinforcement was investigated. Variable parameters included the concrete type (lightweight and conventional), longitudinal bar type (steel and GFRP), and cross section of rebar ( $\rho = 0.75, 1.34\%$ ), as well as the ratio of shear span to effective depth ( $a/d = 2.5$  and 4). Furthermore, the obtained results were compared with those predicted by codes and reliable equations. Based on the analysis and interpretation of the obtained results, the following conclusions can be drawn.

- As expected, all the beams experienced shear failure, which occurred suddenly in most of the beams. In the beams with the shear span-to-effective depth ratio of 4, the number of flexural cracks was significantly larger than that of the beams with the ratio of 2.5.
- The concrete beams reinforced with the GFRP bars showed stiffness less than that of those reinforced with the steel bars, due to a lower modulus of elasticity of the GFRP bars relative to the steel bars.
- For the same  $a/d$  ratio of 2.5, lightweight beams with the GFRP bars had relatively higher shear strength than the beams with steel bars. In this regard, the shear strength of beams G-L-D16-2.5 and S-L-D16-2.5 was 29 and 27 kN, respectively.
- For  $a/d = 4$ , the shear strength of beams made with normal concrete with and reinforced with GFRP bars was higher than the shear strength of the corresponding beams made with lightweight concrete. In this regard, the shear strength of beams G-N-D12-4 and G-L-D12-4 was 28.5 and 15 kN, respectively.

**Table 8** Comparison between experimental results and analytical results obtained from different codes

Beam specimen	Vexp (kN)	The ratio of the experimental value to the predicted value (Vexp/Vpred)			
		ACI 440.1R-06	El-Sayed et al.	JSCE	CAN/CSA-S806-02
G-L-D12-2.5	20	1.55	0.95	1.26	1.17
G-L-D12-4	15	1.26	0.9	1.02	0.96
G-L-D16-2.5	29	1.91	1.24	1.6	1.61
G-L-D16-4	21	1.4	1.05	1.16	0.87
G-N-D12-4	28.5	2.85	1.43	1.96	1.91
G-N-D16-2.5	30	2.38	1.29	1.66	2.01



- In beams with  $\frac{a}{d} = 4$ , it is seen that the shear strength of the beam reinforced with the GFRP bar of the higher cross-sectional area was 40% greater than that of the beam with the GFRP bar of smaller cross-sectional area, while this increase was 45% for the corresponding beams having  $\frac{a}{d} = 2.5$ .
- CSA code showed a good agreement with the experimental results since, in this code, greater attention is paid to the details, which led the theoretical and experimental results to become closer. As the  $\frac{a}{d}$  ratio increases and becomes closer to that of the ordinary beams, the code-proposed equations can predict the shear strength with greater accuracy.

## Compliance with Ethical Standards

**Conflict of interest** The authors declare that they have no conflict of interest.

## References

- ACI-ASCE Committee 326 (1962) Shear and diagonal tension. American Concrete Institute, Farmington Hills
- ACI Committee (2014) ACI 318-14: building code requirements for reinforced concrete. American Concrete Institute, Farmington Hills
- ACI Committee (2015) ACI 440.1R-15: guide for the design and construction of structural concrete reinforced with FRP bars. American Concrete Institute, Farmington Hills
- Akbarzadeh Bengar H (2015) Investigation on behavior of strengthened beams by CFRP in adjacency of columns. *Iran J Struct Eng* 1(2):56–68
- Akbarzadeh Bengar H, Maghsoudi AA (2010) Experimental investigations and verification of debonding strain of RHSC continuous beams strengthened in flexure with externally bonded FRPs. *Mater Struct* 43(6):815–837. <https://doi.org/10.1617/s11527-009-9550-7>
- Akbarzadeh Bengar H, Maghsoudi AA (2011) Flexural strengthening of RC continuous beams using hybrid FRP sheets. In: Ye L, Feng P, Yue Q (eds) *Advances in FRP composites in civil engineering*. Springer, Berlin, pp 739–743. [https://doi.org/10.1007/978-3-642-17487-2\\_163](https://doi.org/10.1007/978-3-642-17487-2_163)
- Akbarzadeh Bengar H, Shahmansouri AA (2020) A new anchorage system for CFRP strips in externally strengthened RC continuous beams. *J Build Eng* 30:101230. <https://doi.org/10.1016/j.jobe.2020.101230>
- Akbarzadeh Bengar H, Hosseinpour M, Celikag M (2020a) Influence of CFRP confinement on bond behavior of steel deformed bar embedded in concrete exposed to high temperature. *Structures* 24:240–252. <https://doi.org/10.1016/j.istruc.2020.01.017>
- Akbarzadeh Bengar H, Shahmansouri AA, Akkas Zangebari Sabet N, Kabirifar K, Tam VWY (2020b) Impact of elevated temperatures on the structural performance of recycled rubber concrete: experimental and mathematical modeling. *Constr Build Mater* 255:119374. <https://doi.org/10.1016/j.conbuildmat.2020.119374>
- Alengaram UJ, Jumaat MZ, Mahmud H, Fayyadh MM (2011) Shear behaviour of reinforced palm kernel shell concrete beams. *Constr Build Mater* 25(6):2918–2927. <https://doi.org/10.1016/j.conbuildmat.2010.12.032>
- Askari Dolatabad Y, Kamgar R, Gouhari Neza I (2019) Rheological and mechanical properties, acid resistance and water penetrability of lightweight self-compacting concrete containing nano-SiO<sub>2</sub>, nano-TiO<sub>2</sub> and nano-Al<sub>2</sub>O<sub>3</sub>. *Iran J Sci Technol Trans Civ Eng*. <https://doi.org/10.1007/s40996-019-00328-1>
- Azarm R, Maheri MR, Torabi A (2017) Retrofitting RC joints using flange-bonded FRP sheets. *Iran J Sci Technol Trans Civ Eng* 41:27–35. <https://doi.org/10.1007/s40996-016-0028-x>
- Bhuvaneshwari P, Mohan KSR (2017) Strength analysis of reinforced concrete beams affected by fire using glass fiber sheet and PP fiber ECC as binders. *Iran J Sci Technol Trans Civ Eng* 41:37–47. <https://doi.org/10.1007/s40996-016-0029-9>
- Bompa DV, Elghazouli AY (2015) Ultimate shear behaviour of hybrid reinforced concrete beam-to-steel column assemblages. *Eng Struct* 101:318–336. <https://doi.org/10.1016/j.engstruct.2015.07.033>
- BSI (1997) BS 8110-1: structural use of concrete. British Standard Institution, London
- Campana S, Fernández Ruiz M, Anastasi A, Muttoni A (2013) Analysis of shear-transfer actions on one-way RC members based on measured cracking pattern and failure kinematics. *Mag Concr Res* 65(6):386–404. <https://doi.org/10.1680/macrc.12.00142>
- Canadian Standards Association (2016) Design and construction of building components with fibre-reinforced polymers. Canadian Standards Association, Toronto
- CEN European Committee for Standardization (2004) EN 1992-1-1, Eurocode 1: design of concrete structures. BSI British Standards, Brussels
- Chung S-Y, Elrahman MA, Stephan D (2018) Effects of expanded polystyrene (EPS) sizes and arrangements on the properties of lightweight concrete. *Mater Struct* 51:57. <https://doi.org/10.1617/s11527-018-1182-3>
- Dhahir MK (2017) Shear strength of FRP reinforced deep beams without web reinforcement. *Compos Struct* 165:223–232. <https://doi.org/10.1016/j.compstruct.2017.01.039>
- El-Sayed AK, El-Salakawy EF, Benmokrane B (2006) Shear strength of FRP-reinforced concrete beams without transverse reinforcement. *ACI Struct J* 103:235. <https://doi.org/10.14359/15181>
- Farrokh Ghatte H (2020) External steel ties and CFRP jacketing effects on seismic performance and failure mechanisms of substandard rectangular RC columns. *Compos Struct* 248:112542. <https://doi.org/10.1016/j.compstruct.2020.112542>
- Farrokh Ghatte H, Comert M, Demir C, Akbaba M, Ilki A (2019) Seismic retrofit of full-scale substandard extended rectangular RC columns through CFRP jacketing: test results and design recommendations. *J Compos Constr* 23(1):04018071. [https://doi.org/10.1061/\(ASCE\)CC.1943-5614.0000907](https://doi.org/10.1061/(ASCE)CC.1943-5614.0000907)
- GangaRao HV, Taly N, Vijay P (2006) Reinforced concrete design with FRP composites. CRC Press, Boca Raton. <https://doi.org/10.1201/9781420020199>
- Ghasemi S, Maghsoudi AA, Akbarzadeh Bengar H, Ronagh HR (2015) Flexural strengthening of continuous unbonded post-tensioned concrete beams with end-anchored CFRP laminates. *Struct Eng Mech* 53:1083–1104. <https://doi.org/10.12989/sem.2015.53.6.1083>
- Gonen T (2015) Mechanical and fresh properties of fiber reinforced self compacting lightweight concrete. *Sci Iran* 22:313–318
- Hajiloo H, Green MF, Gales J (2018) Mechanical properties of GFRP reinforcing bars at high temperatures. *Constr Build Mater* 162:142–154. <https://doi.org/10.1016/j.conbuildmat.2017.12.025>
- Hosseinpour M, Celikag M, Akbarzadeh Bengar H (2019) Strengthening and shape modification of fire-damaged concrete with expansive cement concrete and CFRP wrap. *Sci Iran* 26:699–708. <https://doi.org/10.24200/sci.2017.4592>

- JSCE (1997) Recommendation for design and construction of concrete structures using continuous fiber reinforcing materials. Concrete engineering series 23. Japan Society of Civil Engineers, Tokyo
- Jumaat MZ, Alengaram UJ, Mahmud H (2009) Shear strength of oil palm shell foamed concrete beams. *Mater Des* 30(6):2227–2236. <https://doi.org/10.1016/j.matdes.2008.09.024>
- Kaveh A, Bakhshpoori T, Hamze-Ziabari S (2017) New model derivation for the bond behavior of NSM FRP systems in concrete. *Iran J Sci Technol Trans Civ Eng* 41:249–262. <https://doi.org/10.1007/s40996-017-0058-z>
- Leonhardt F (1970) Shear and torsion in pre-stressed concrete. Paper presented at the 6th FIP Congress, Prague
- Limbachiya M, Meddah MS, Ouchagour Y (2012) Performance of Portland/silica fume cement concrete produced with recycled concrete aggregate. *ACI Mater J*. <https://doi.org/10.14359/51683574>
- Maghsoudi AA, Akbarzadeh Bengar H (2011a) Acceptable lower bound of the ductility index and serviceability state of RC continuous beams strengthened with CFRP sheets. *Sci Iran* 18:36–44. <https://doi.org/10.1016/j.scient.2011.03.005>
- Maghsoudi AA, Akbarzadeh Bengar H (2011b) Moment redistribution and ductility of RHSC continuous beams strengthened with CFRP. *Turk J Eng Environ Sci* 33(1):45–59. <https://doi.org/10.3906/muh-0901-6>
- Mousavinejad SHG, Sara YGS (2019) Experimental study effect of silica fume and hybrid fiber on mechanical properties lightweight concrete. *Iran J Sci Technol Trans Civ Eng* 43:263–271. <https://doi.org/10.1007/s40996-018-0137-9>
- Naseri H, Danesh M, Naseri M (2019) An experimental investigation into fiber/textile-reinforced lightweight concrete precast panels for temporary housing. *Iran J Sci Technol Trans Civ Eng* 1:1–8. <https://doi.org/10.1007/s40996-019-00243-5>
- Nematzadeh M, Shahmansouri AA, Fakoor M (2020) Post-fire compressive strength of recycled PET aggregate concrete reinforced with steel fibers: optimization and prediction via RSM and GEP. *Constr Build Mater* 252:119057. <https://doi.org/10.1016/j.conbuildmat.2020.119057>
- Nilson AH, Martinez S (1986) Mechanical properties of high-strength lightweight concrete. In: *Journal proceedings*, vol 4, pp 606–613. <https://doi.org/10.14359/10454>
- Omeman Z, Nehdi M, El-Chabib H (2008) Experimental study on shear behavior of carbon-fiber-reinforced polymer reinforced concrete short beams without web reinforcement. *Can J Civ Eng* 35:1–10. <https://doi.org/10.1139/L07-080>
- Oskouei AV, Kivi MP, Araghi H, Bazli M (2017) Experimental study of the punching behavior of GFRP reinforced lightweight concrete footing. *Mater Struct* 50:256. <https://doi.org/10.1617/s11527-016-0971-9>
- Real S, Bogas JA, Ferrer B (2017) Service life of reinforced structural lightweight aggregate concrete under chloride-induced corrosion. *Mater Struct* 50:101. <https://doi.org/10.1617/s11527-016-0971-9>
- Said M, Adam MA, Mahmoud AA, Shanour AS (2016) Experimental and analytical shear evaluation of concrete beams reinforced with glass fiber reinforced polymers bars. *Constr Build Mater* 102:574–591. <https://doi.org/10.1016/j.conbuildmat.2015.10.185>
- Saleh N, Ashour A, Lam D, Sheehan T (2019) Experimental investigation of bond behaviour of two common GFRP bar types in high-strength concrete. *Constr Build Mater* 201:610–622. <https://doi.org/10.1016/j.conbuildmat.2018.12.175>
- Shafigh P, Mahmud HB, Jumaat MZB, Ahmmad R, Bahri S (2014) Structural lightweight aggregate concrete using two types of waste from the palm oil industry as aggregate. *J Clean Prod* 80:187–196. <https://doi.org/10.1016/j.jclepro.2014.05.051>
- Shayanfar J, Akbarzadeh Bengar H (2018) A practical model for simulating nonlinear behaviour of FRP strengthened RC beam-column joints. *Steel Compos Struct* 27:49–74. <https://doi.org/10.12989/scs.2018.27.1.049>
- Shoaib A, Lubell AS, Bindiganavile VS (2015) Shear response of lightweight steel fiber reinforced concrete members without stirrups. *Mater Struct* 48:3141–3157. <https://doi.org/10.1617/s11527-014-0387-3>
- Singh SB (2015) Analysis and design of FRP reinforced concrete structures. McGraw Hill Professional, New York
- Tang CW, Yen T, Chen HJ (2009) Shear behavior of reinforced concrete beams made with sedimentary lightweight aggregate without shear reinforcement. *J Mater Civ Eng* 21(12):730–739. [https://doi.org/10.1061/\(ASCE\)0899-1561\(2009\)21:12\(730\)](https://doi.org/10.1061/(ASCE)0899-1561(2009)21:12(730))
- Tureyen AK, Frosch RJ (2002) Shear tests of FRP-reinforced concrete beams without stirrups. *ACI Struct J* 99:427–434. <https://doi.org/10.14359/12111>
- Wu C, Bai Y, Kwon S (2016) Improved bond behavior between GFRP rebar and concrete using calcium sulfoaluminate. *Constr Build Mater* 113:897–904. <https://doi.org/10.1016/j.conbuildmat.2016.03.132>
- Xu B, Bompa DV, Elghazouli AY, Ruiz-Teran AM, Stafford PJ (2018) Behaviour of rubberised concrete members in asymmetric shear tests. *Constr Build Mater* 159:361–375. <https://doi.org/10.1016/j.conbuildmat.2017.10.091>
- Yazdanbakhsh A, Tian Y (2019) Shear performance of reinforced concrete beams incorporating stiff slender elements. *Constr Build Mater* 222:263–277. <https://doi.org/10.1016/j.conbuildmat.2019.06.158>
- Yazdani N, Goucher E (2015) Increasing durability of lightweight concrete through FRP wrap. *Compos Part B Eng* 82:166–172. <https://doi.org/10.1016/j.compositesb.2015.08.036>
- Zhang L, Sun Y, Xiong W (2015) Experimental study on the flexural deflections of concrete beam reinforced with Basalt FRP bars. *Mater Struct* 48:3279–3293. <https://doi.org/10.1617/s11527-014-0398-0>
- Zhou J, Shen W, Wang S (2017) Experimental study on torsional behavior of FRC and ECC beams reinforced with GFRP bars. *Constr Build Mater* 152:74–81. <https://doi.org/10.1016/j.conbuildmat.2017.06.131>